Dasatinib Modulates Invasive and Migratory Properties of Canine Osteosarcoma and has Therapeutic Potential in Affected Dogs

Kevin Marley, Justine Gullaba[1], Bernard Seguin[2], Howard B. Gelberg and Stuart C. Helfand

Department of Clinical Sciences Oregon State University, 105 Magruder Hall, Corvallis OR, 97331, USA

Abstract

BACKGROUND: This investigation sought to elucidate the relationship between hepatocyte growth factor (HGF)–induced metastatic behavior and the tyrosine kinase inhibitors (TKIs) crizotinib and dasatinib in canine osteosarcoma (OS). Preliminary evidence of an apparent clinical benefit from adjuvant therapy with dasatinib in four dogs is described. *METHODS:* The inhibitors were assessed for their ability to block phosphorylation of MET; reduce HGF-induced production of matrix metalloproteinase (MMP); and prevent invasion, migration, and cell viability in canine OS cell lines. Oral dasatinib (0.75 mg/kg) was tested as an adjuvant therapy in four dogs with OS. *RESULTS:* Constitutive phosphorylation of MET was detected in two cell lines, and this was unaffected by 20-nM incubation with either dasatinib or crizotinib. Incubation of cell lines with HGF (MET ligand) increased cell migration and invasion in both cell lines and increased MMP-9 activity in one. Dasatinib suppressed OS cell viability and HGF-induced invasion and migration, whereas crizotinib reduced migration and MMP-9 production but did not inhibit invasion or viability. *CONCLUSIONS:* Invasion, migration, and viability of canine OS cell lines are increased by exogenous HGF. HGF induces secretion of different forms of MMP in different cell lines. The HGF-driven increase in viability and metastatic behaviors we observed are more uniformly inhibited by dasatinib. These observations suggest a potential clinical benefit of adjuvant dasatinib treatment for dogs with OS.

Translational Oncology (2015) 8, 231–238

Introduction

The receptor tyrosine kinase (RTK) MET is considered a growth and motility factor because it provides crucial signals for survival and migration during embryogenesis [1]. MET signaling is normally initiated by binding its ligand, hepatocyte growth factor (HGF, also known as scatter factor), but may be constitutively activated as a consequence of point mutations, coexpression with HGF in the same tissue, or overexpression [2]. Deregulation of MET is associated with transformation and metastatic progression in many cancers, and this has led to research of the MET pathway as a therapeutic target [3,4]. Anti-MET strategies have been investigated using antibodies [5], decoy receptors [6], and a variety of tyrosine kinase inhibitors (TKIs) [7–10].

MET is expressed in a variety of tissues including canine osteosarcoma (OS) tumors and cell lines [11]. The MET-specific TKI crizotinib, when tested against human OS cell lines, was able to selectively induce apoptosis, inhibit cell growth *in vitro*, and prevent tumor growth in a mouse xenograft model [10]. The overexpression and coexpression of MET and HGF in canine OS suggest autocrine

or paracrine activation and indicate that MET may be an important target in this neoplasm [12,13]. In this regard, short interfering RNA against MET reduced motility and invasion *in vitro*[13]; but the MET-specific TKI, PHA-665752, had no effect on viability in canine OS cells expressing high levels of MET [13]. This suggests the MET

Address all correspondence to: Stuart C. Helfand or Kevin Marley, Department of Clinical Sciences Oregon State University, 105 Magruder Hall, Corvallis Oregon, 97331, USA.
E-mail: sch_726@yahoo.com (Stuart C. Helfand), kevin.marley@oregonstate.edu (Kevin Marley)
[1]Present address: Purdue University College of Veterinary Medicine, 625 Harrison St, West Lafayette, IN, 47907, USA.
[2]Present address: Flint Animal Cancer Center, Department of Clinical Sciences Colorado State University, Fort Collins, Colorado, 80525, USA.

pathway, in some cases, may act independently from those that modulate cell survival; and this could be important to the study of metastatic behavior in tumor cells.

Metastatic tumor cells may have hijacked the MET pathway to increase their ability to invade surrounding tissue [14]. This complicated process likely involves coordinated changes in cell-to-cell signaling, the induction of contact independence, and the production of proteases, such as matrix metalloproteinase, that degrade extracellular matrix [15]. In the current study, the MET pathway was investigated in canine OS in the context of invasive behavior, including matrix metalloproteinase (MMP) activity induced by exogenous HGF. The TKIs crizotinib and dasatinib were tested for their ability to reduce cell viability, prevent invasion and migration, and block MMP activity in the presence and absence of HGF. In addition, our previous work identified dasatinib as a potential treatment for canine OS [16]. Although MET has not been identified as a specific target of dasatinib, dasatinib has been reported to block invasion, migration, and proliferation in a variety of human sarcoma cell lines including OS [17]. Herein we report the apparent extended survival of a cohort of four dogs with OS that were treated with dasatinib.

Methods

Cell Lines and Reagents

Two canine OS cell lines, COS [18] and Clone-4 developed in our laboratory (BS), were used in this study. Cells were cultured at 37°C in a humidified 5% CO_2 atmosphere. Cell culture medium was RPMI 1640 supplemented with 2 mM glutamine, 2 mM sodium pyruvate, 2 mM HEPES, 1% penicillin-streptomycin, and 10% FBS, hereafter referred to as *R10*. Serum-free medium referred to as *R0* was identical except that it contained no FBS. Recombinant baculovirus canine HGF (rcHGF) was purchased from R&D Systems (Minneapolis, MN). Cells were detached with 0.25% trypsin and 0.03% EDTA solution, and counted on a hemocytometer to assess cell numbers before use.

Invasion Assay

Invasion studies were performed using 8-μm pore size, reduced growth factor, Matrigel Invasion Chambers (BD Biosciences, Bedford, MA) according to the manufacturer's instructions. Briefly, cells were seeded at a density of 25,000/well into the top chamber in R0 medium. The bottom chambers contained R10 medium. HGF or TKI was added to both the top and bottom chambers when appropriate, so the only difference between the top and bottom chambers was the 10% serum. After 24 hours, the membranes were removed, stained with Diff Quik, mounted on glass slides, and imaged on a microscope. All cells that had migrated through each membrane were counted, and each experiment was repeated at least twice.

Migration Assay

Cells were seeded into six-well plates (2×10^5 cells/well) in 2 mL of R10 medium and allowed to adhere overnight. The following day, the R10 medium was replaced with R0; and the cells were again incubated overnight. After 24 hours, the medium was removed and replaced as described in each figure; and a sterile pipette tip was used to scratch two intersecting lines in a cross configuration into the subconfluent cells. The plates were imaged immediately using a microscope with attached digital camera (Nikon Eclipse *ti*). After 20 hours, the scratched sections were imaged again; and cells that had

migrated into the previously clear zones were counted manually. To accomplish this task, identically sized boxes were overlaid onto each image using photo processing software (Adobe Photoshop); and all cells within these were counted. The crosshatch pattern was used to place the counting box in a similar location for every condition. Each of these assays was repeated at least twice, and data represent the mean of two independent assays.

Vital Staining

Cells prepared as described for migration assays (above) were incubated with 0 to 40 nM dasatinib for 24 hours and then trypsinized, exposed to trypan blue, and counted in a hemocytometer. Cells that showed a deep blue color were considered dead. The incubation medium was added back to the trypsinized cells before counting to account for floating cells. Data shown are means ± SD of two independent experiments.

Cell Viability

Cells were seeded in 96-well plates at a density of 5000 cells/well in a volume of 100 μL of R10 and allowed to adhere overnight. The following day, the R10 medium was replaced with R0; and the cells were again incubated overnight. The medium was then replaced with fresh R0 medium containing various concentrations of TKI plus or minus 20 ng/mL of HGF. Cell viability was assessed after 48 hours using an 3-(4,5-dimethylthiazol-2-yl)-5-(3-carboxymethoxyphenyl)-2-(4-sulfophenyl)-2H-tetrazolium (MTS) assay according to the manufacturer's instructions (Promega, #G3580). All data are expressed as means ± SD of triplicate wells and are representative of three independent experiments.

Flow Cytometry

Flow cytometry was used to detect binding of annexin V to phosphotidyl serine on the surface of cells in early apoptosis and propidium iodide to DNA in late-stage apoptosis or dead cells. Cells were serum-starved overnight in R0 medium then incubated in the same medium with 0 or 20 nM dasatinib ± HGF (20 ng/mL) for 24 hours. After incubation, the media were collected and the cells collected using 0.005% trypsin in PBS. The incubation media containing cells that were released from the flask were then added back to the trypsinized cells along with a 100-μL aliquot of serum to stop the trypsin. Cells were then reacted with biotinylated annexin V-FITC and propidium iodide using a commercially available kit (Calbiochem). A minimum of 20,000 cells per sample was collected on a Beckman Coulter FC-500 flow cytometer. Data analysis and software compensation were performed using WinList (Verity Software, Topsham, ME). Annexin V (FITC) and propidium iodide fluorescence intensity were gated on forward and side scatter to exclude cell debris. Spectral overlap was compensated using single-stain controls.

Western Blots

Cells were seeded (3×10^6/well) in 25-cm^2 flasks and allowed to adhere overnight before incubation with dasatinib or crizotinib in the presence or absence of HGF. At the end of the incubation period, the media and cells were removed using a cell scraper; and the cells were pelleted in a tabletop centrifuge (3 minutes, 450g). The supernatants were discarded, and cell pellets were extracted in 50-μL ice-cold radioimmunoprecipitation buffer with added protease and phosphatase inhibitor cocktail (Thermo Scientific, Rockford, IL). Extracts were sonicated 4 × 1 second using an ultrasonic dismembranator (Fisher, Model 150T) and pelleted at 10,000g to remove cellular
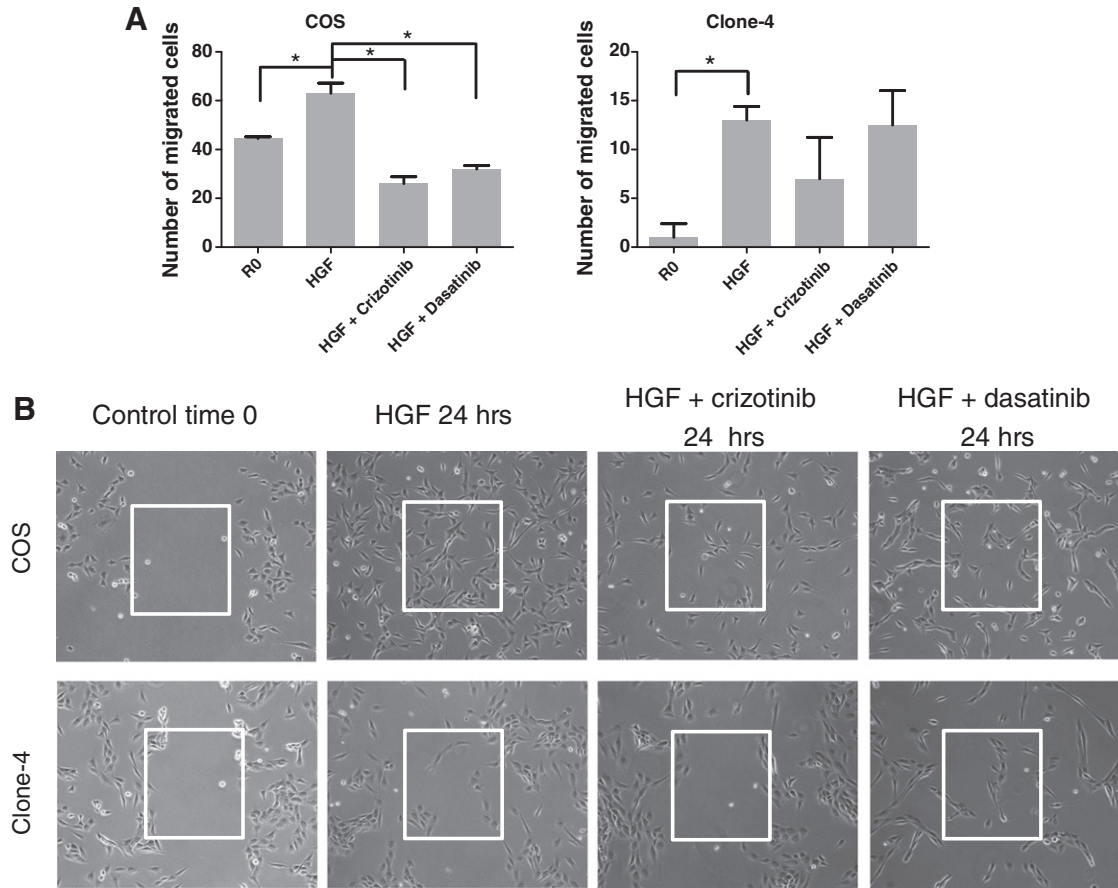
Figure 1. Migration assay. (A) HGF increased migration in both cell lines, but the TKIs crizotinib and dasatinib were able to suppress migration only in the COS cell line. *$P \leq .05$. Data are representative of three independent experiments. (B) Representative photomicrographs of cells treated with HGF ± TKIs. After 24 hours, cells that migrated into the box overlay were counted (data shown in A).

debris. Protein concentration was measured using a Bradford assay (Pierce, Rockford, IL). Proteins (20 μg/lane) were separated on 4% to 12% SDS polyacrylamide gels and transferred to polyvinylidene
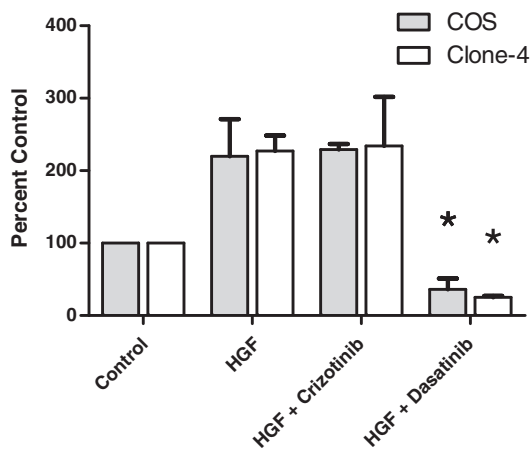
difluoride membranes using standard methods as follows. The membranes were blocked in 2.5% albumin and reacted with indicated primary antibodies diluted 500:1 for 3 hours at room temperature or overnight at 4°C. The phospho-Met (Y1230/Y1234/Y1235) antibody used was a rabbit polyclonal purchased from Millipore (Billerica, MA). Total MET and actin antibodies were purchased from Santa Cruz Biotechnology (Santa Cruz, CA). The membranes were washed, reacted with horseradish peroxidase–linked secondary antibody (Santa Cruz Biotechnology) diluted 30,000:1, and exposed to substrate (GE Healthcare).

Zymography

Cells were seeded at a density of 3000 cells/well in 24-well plates and allowed to adhere overnight. The following day, the growing cells were serum starved for 24 hours and then incubated for 24 hours in 500 μL of R0 medium plus or minus either TKI at a concentration of 20 nM plus or minus HGF (20 ng/mL). After incubation, an aliquot of medium was removed and centrifuged at 10,000g for 10 minutes to remove debris. A 10-μL aliquot of each of these was separated by electrophoresis on 10% polyacrylamide gelatin zymogram gels according to the manufacturer's directions (Invitrogen, Carlsbad, CA). Following electrophoresis, the gels were incubated in developing solution for 20 hours at 37°C, stained with Coomassie Blue (G-BioSciences, St. Louis, MO), and imaged with a digital camera (LAS 4000; GE Healthcare, Buckinghamshire, UK). Densitometry
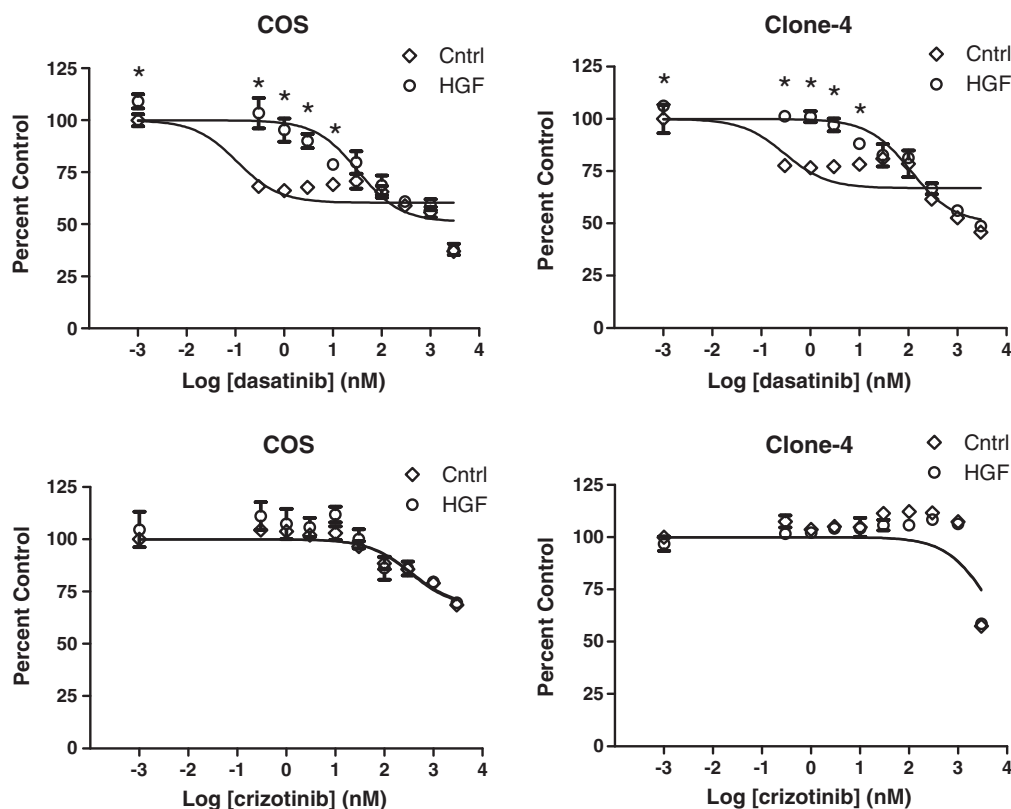

Figure 2. Invasion assay. HGF increased invasion in both cell lines, and this increase was prevented by dasatinib but not crizotinib. *$P \leq .05$, different from HGF treated. Data are presented as means ± SE of duplicate assays and are representative of three independent assays.

Figure 3. MTS assays with tyrosine kinase inhibitors and HGF. Viability of HGF-stimulated cells was inhibited at low concentrations by dasatinib (top panels) but not by crizotinib (bottom panels). *Difference between HGF-treated and control at the same TKI concentration ($P \le .05$). IC50 values for dasatinib were 0.1 nM in controls and 32 nM in cells incubated with HGF in the COS cell line. These values were 0.3 nM and 112 nM in the Clone-4 cell line, respectively. IC50 values for crizotinib were 340 nM and 357 for COS controls and HGF-treated cells and was not reached in the Clone-4 cell line.

for these and the Western blot images was performed using Image Quant TL software (GE Healthcare).

Histopathology

Biopsy samples of the proximal tibia were decalcified, sectioned, and stained with hematoxylin and eosin using standard methods.

Statistics

Statistical comparisons using analysis of variance with Tukey *post hoc* tests were performed, when appropriate, using Graphpad Prism software (La Jolla, CA). Nonlinear regression using log-transformed values were used to calculate IC50s from the MTS assay results using the same software.
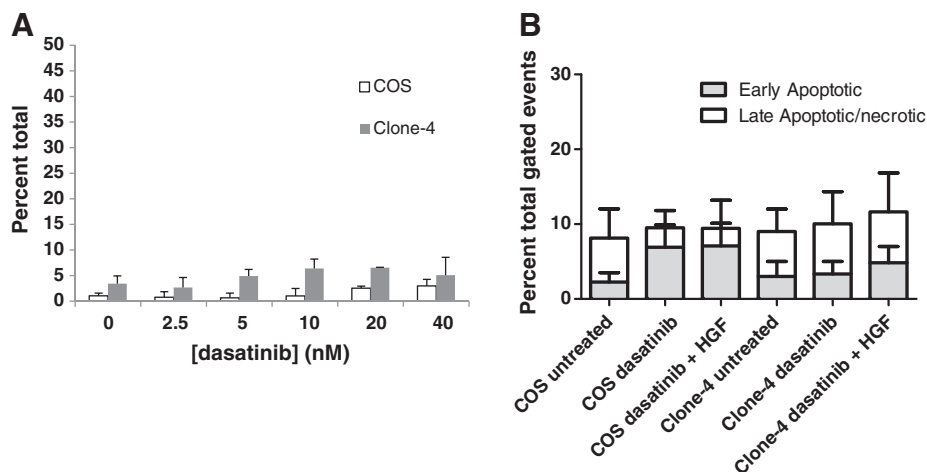

Figure 4. Cell death/apoptosis. (A) Trypan blue, live/dead, cell assay of COS and Clone-4 cells incubated 24 hours in 0- to 40-nM concentrations of dasatinib shows no significant increase in cell death due to TKI treatment ($P > .05$). Data shown are means ± SD of two independent experiments. (B) Flow cytometry data from cells incubated for 24 hours with 20 nM dasatinib show no increase in combined level of early apoptotic or late apoptotic/necrotic cells ($P > .05$). Data shown are means ± SD of two independent experiments.
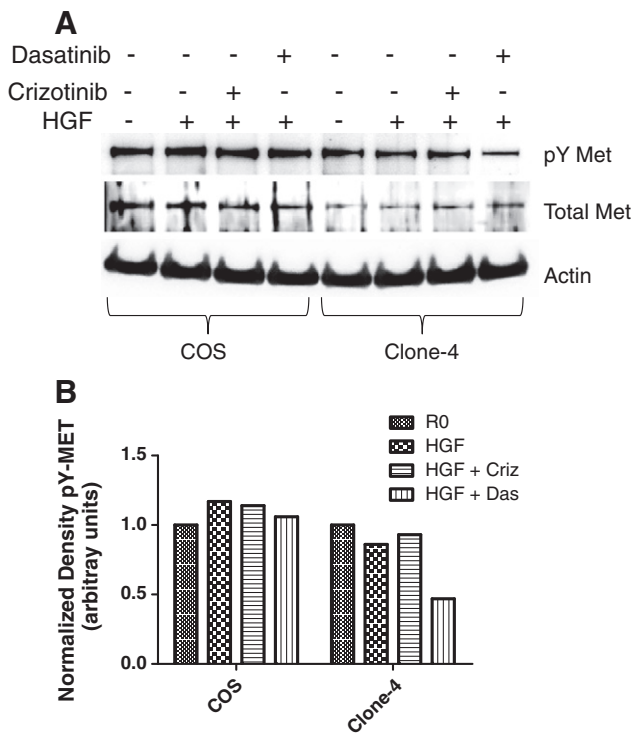
Figure 5. MET activation. (A) Western blots from serum-starved cells show that MET is constitutively activated in both cell lines. HGF incubation had little effect on MET phosphorylation at tyrosines 1230/1234/1235, and TKI incubation (20 nM) was not sufficient to reverse this. Dasatinib suppressed but did not eliminate the pY-MET signal in Clone-4 cells. (B) Histogram of densitometry of pY-MET Western blot shown in A.

Figure 6. Expression and protease activity of MMP2 in COS and Clone-4 cells exposed to HGF and crizotinib or dasatinib. (A) Cells were incubated overnight in R10 media (10% serum) or serum-free media with HGF ± TKI as indicated. Criz-20 and criz-40 indicate 20-nM and 40-nM incubation concentrations. The expression patterns between the two cell lines are quite different, with COS cells expressing the pro- and active form uniformly, whereas the Clone-4 cells expressed only the active form. The protease activity of active MMP2 was reduced by both crizotinib and dasatinib, with dasatinib appearing to be the more effective drug at these low concentrations.

Results

Migration/Invasion

HGF caused an increase in migration in serum-starved canine OS cells ($P \leq .05$, Figure 1), and low-concentration (20 nM) TKI incubation suppressed migration in COS but not Clone-4 cells. The increase in migration attributed to HGF was significant in both cell lines, but the rate of migration of the Clone-4 cells was much lower (Figure 1). HGF-induced invasion was more consistent and was more than 100% greater than controls in both cell lines ($P < .05$, Figure 2). The TKIs' ability to prevent this increase was specific only to dasatinib. In fact, dasatinib not only prevented the HGF-induced increase but reduced overall invasion from 205 to 25% of that seen in the serum-starved and untreated cells (Figure 2).

Cell Viability

Low-concentration dasatinib, but not crizotinib, reduced the viability of serum-starved OS cells (Figure 3). This effect was blocked by HGF in both cell lines at TKI concentrations less than 100 nM. The protective effect of HGF was lost at dasatinib concentrations greater than 100 nM. Crizotinib was less effective and only slightly inhibited viability of the COS cells at concentrations of 100 nM and greater (Figure 3). Crizotinib had no effect on the Clone-4 cell line at concentrations less than 3 μM, which was the highest concentration deemed reasonable in this study. No significant changes in cell death or apoptosis were attributable to 20-nM dasatinib incubation (Figure 4), which was the concentration used for the migration and
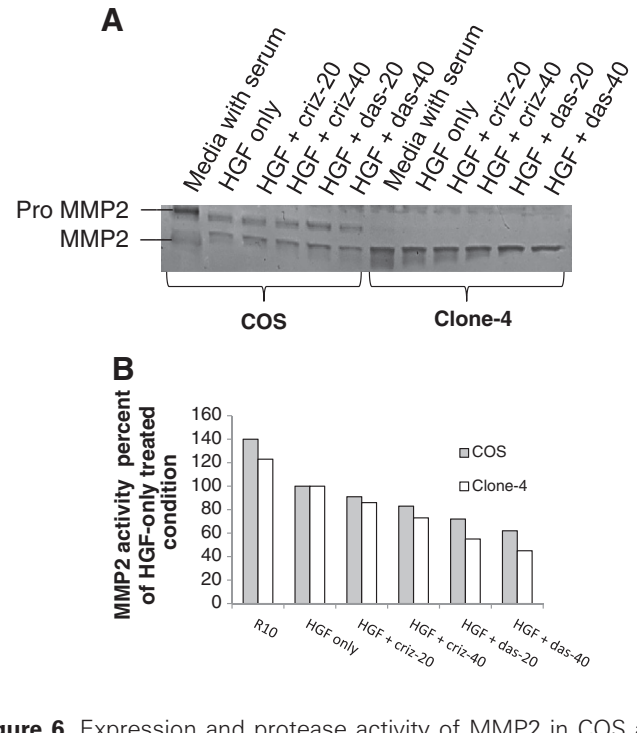
invasion assays. Under serum-starved conditions, the dasatinib IC50 values for the COS cell line were 0.1 nM for the untreated and 32 nM for the HGF-treated cells. Dasatinib was similarly effective in the Clone-4 cell line, with IC50s of 0.3 nM and 112 nM in the untreated and treated cells, respectively. The crizotinib IC50s for the COS cells were 340 nM and 357 nM for the untreated and HGF-treated cells, respectively; and no IC50 values were observed for crizotinib in the Clone-4 cell because the drug did not effectively reduce viability in these cells.

MET Phosphorylation

Tyrosine phosphorylation (pY) of MET in serum-starved cells was strongly positive and appeared unchanged by HGF (Figure 5). TKI incubation similarly appeared to have little effect on pY-MET with the exception that dasatinib was able to reduce, but not eliminate, this activation signal in the Clone-4 cells.

Effects of HGF and TKIs on MMP-2 and MMP-9

This study assessed the effects of HGF on MMP-2 and MMP-9 secretion by OS cell lines and measured the ability of the TKIs dasatinib and crizotinib to block this secretion. We were surprised by the observation that MMP isoform production was dramatically different in the two OS cell lines. Beginning with MMP-2, secretion of the pro-form of MMP-2 was dramatically induced in the COS cells by serum-containing media; but this was not observed in the Clone-4
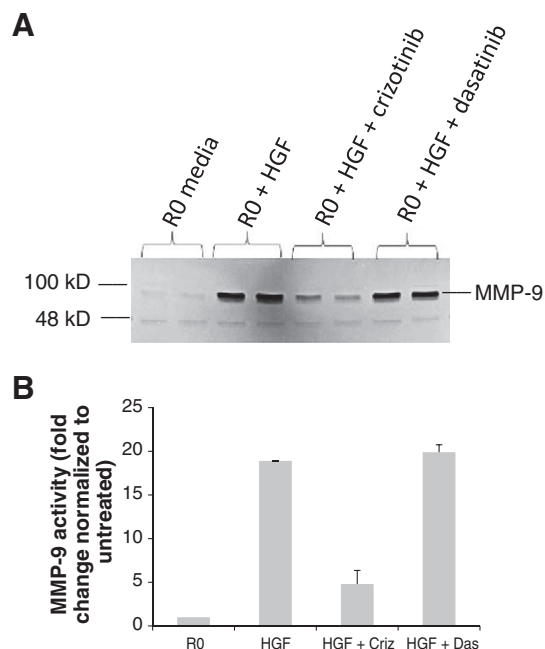
A

B

Figure 7. Expression and protease activity of MMP9 in COS cells exposed to HGF and crizotinib or dasatinib. (A) Zymogram showing the result of two independent experiments ran on the same gel. (B) Densitometry histogram of data from zymogram shown in A. Error bars indicate SD.

cells (Figure 6). Both the pro- and active forms of MMP-2 were produced in the presence of HGF in the COS cells, but HGF induced only the active form in the Clone-4 cells. The zymogram densitometry shows a dose–response relationship, with both TKIs suppressing secretion of the active form of MMP-2; however, this effect was more pronounced with dasatinib (Figure 6). The difference between the two cell lines was more pronounced with MMP-9 secretion versus that seen in MMP-2, as media from the COS cells produced a major band on the zymographs, whereas none was detected using media from the Clone-4 cell line. In this regard, the MMP-9 secretion was entirely dependent on HGF in the COS cells (Figure 7, MMP-9 data for Clone-4 are not shown). This HGF-induced MMP-9 secretion was suppressed in COS cells by coincubation with crizotinib but not dasatinib. Data shown are representative of three independent experiments (Figure 7).

Clinical Correlates

We have treated dogs with dasatinib for appendicular OS with owner consent. This was combined with limb amputation and carboplatin chemotherapy, which are among the current standard-of-care treatments for canine OS. Although not a clinical trial, we felt that it was important to determine if our *in vitro* data had the potential to be translated into affected dogs in a pilot data setting. This afforded the opportunity to gain experience on tolerable drug dosing, establish a protocol for a future clinical trial, and begin to generate observations of a potential therapeutic role for dasatinib in dogs with OS.

The starting dose of dasatinib in all dogs has been 0.5 mg/kg given every day or every other day (Table 1). Oral antiemetics were given on treatment days if needed (maropitant 2 mg/kg once and/or ondansetron 0.2 mg/kg two to three times a day). The primary adverse effects have

been inappetence and gastrointestinal upset with diarrhea. In most cases, this has not precluded dasatinib treatment. After 2 weeks without significant adverse effects, the 0.5-mg/kg dose was increased to 0.75 mg/kg and continued indefinitely or until the owner's decision to stop. Doses higher than 0.75 mg/kg were generally not tolerated. Table 1 contains details of the dogs' signalment, tumor location, treatments, and survival times. Two dogs' tumors had been profiled against a panel of drugs, and dasatinib was predicted to be the most effective in these animals. These dogs had the longest survival times (Table 1). Details have been previously published for the golden retriever in the table [16]. The dogs in this report were all of large stature, which is typical of canine and human OS patients. All developed OS in the proximal tibia, a common site for OS in humans, whereas the distal radius is the most common site in the dog. Histopathological examination by a board-certified veterinary pathologist confirmed the diagnosis of OS in each dog's tumor. Representative histological sections from the tibial OS of the Great Pyrenees (Table 1) are shown in Figure 8(*A* and *B*). The radiographic image of this tumor is shown in Figure 8(*C*). It is primarily an osteolytic tumor with destruction of bone within the medullary space and a pathological fracture of the cortex (Figure 8*C*, lower arrow).

Three of the four dogs commenced dasatinib treatment after limb amputation and five cycles of carboplatin chemotherapy given every 3 weeks at standard dosing (300 mg/m^2). Dasatinib treatment was begun 3 weeks after completion of chemotherapy. The dogs were free of radiographically detectable pulmonary metastases at that time. The longest surviving dog (German Shepherd mix, Table 1) started dasatinib when pulmonary metastases were detected after three of five planned carboplatin treatments. A single (1 cm) pulmonary nodule (Figure 8*D*) appeared to resolve after 3 months dasatinib treatment (Figure 8*E*). This dog did not receive any additional carboplatin chemotherapy but continued on dasatinib for a total of 25 months. Thus, our preliminary radiographic evidence suggests that dasatinib stabilized or induced partial remission of pulmonary metastases in at least two dogs.

The shortest survival time of any of the four dogs treated with adjuvant dasatinib was nearly 1.5 times as long as dogs noted in the historical reports; and one dog, as of this writing, continues to be alive 33 months after diagnosis (>3.2 times longer than the reported median survival time).

Discussion

This study investigated the role of HGF in canine OS using an *in vitro* model of metastasis because metastasis, not the primary tumor, is the cause of mortality in OS. We describe effects of the TKIs crizotinib and dasatinib using this model system and include

Table 1. Patient Characteristics, Survival and Treatments

Dog Signalment	Tumor Location	Survival Time	Dasatinib Treatment
Golden Retriever 7 y old, MN	Left proximal tibia	29 mo*	0.5-0.75 mg/kg Q24 6.5 mo
Labrador Retriever 4 y old, MN	Left proximal tibia	28 mo*	0.5-0.75 mg/kg EOD 10 mo
German Shepherd mix 9 y old, MN	Right proximal tibia	33 mo; still living	0.5-0.75 mg/kg Q24 25 mo
Great Pyrenees 10 y old, MN	Right proximal tibia	15 mo*	0.5-0.75 mg/kg EOD 7 mo

Q24, every 24 hours; *EOD*, every other day; *MN*, male neutered.
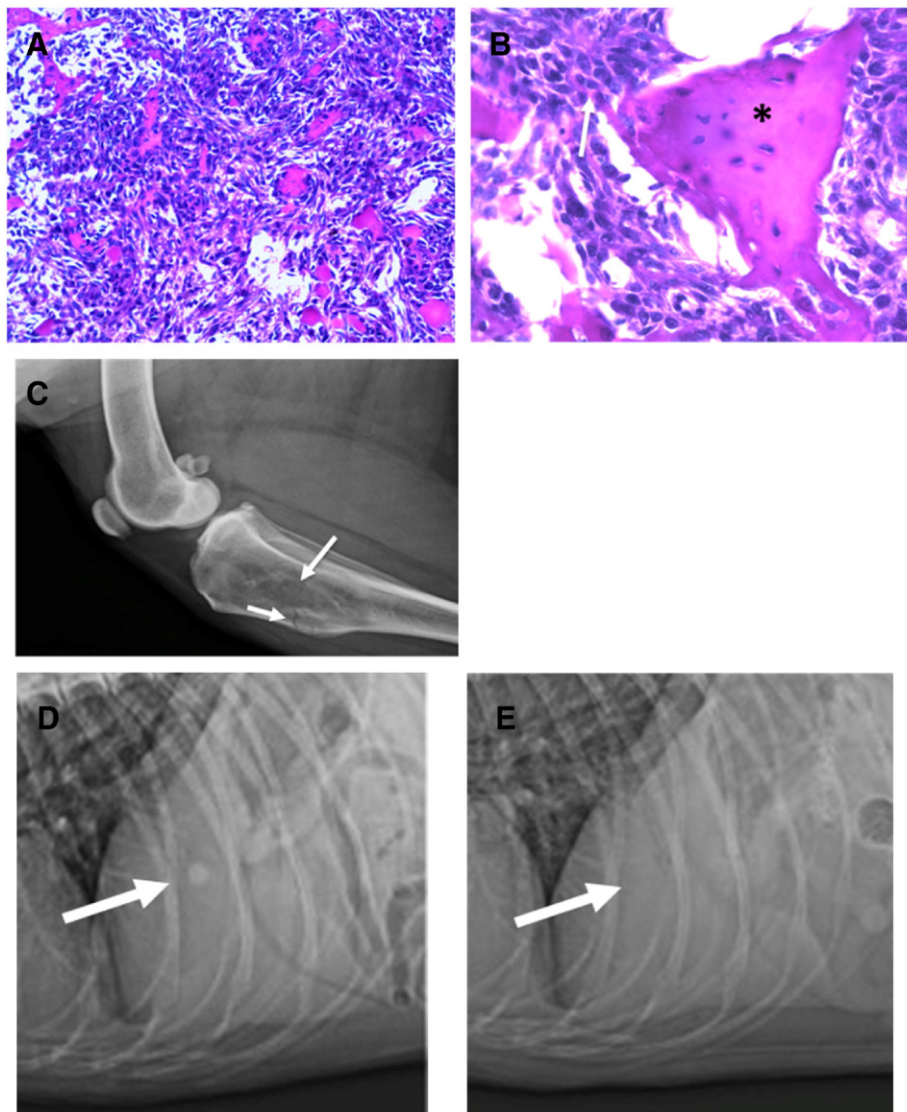* Death due to metastatic disease.

Figure 8. Case studies. (A) Histopathology of right tibial OS from the Great Pyrenees shows that the medullary cavity was invaded by streams of tightly-packed, infiltrating, spindloid cells. These cells had fibrillar, eosinophilic, indistinctly-bordered cytoplasm and elongate nuclei with undulant membranes, coarse, dispersed chromatin, and multiple nucleoli. (B) The cells became more rounded (arrow) along seams of osteoid (asterisk) where they were trapped in lacunae. Multinucleated cells were present and there was 1 mitotic figure in 10 contiguous $400 \times$ fields. (A) $200 \times$, (B) $400 \times$. (C) Radiographic image (lateral view) of the Great Pyrenees' tibia shows marked destruction of bone within the medullary space giving the appearance of patchy bone loss (top arrow). There is a pathological fracture of the cortex (lower arrow). (D) Radiographic image of lung metastasis that appeared resolved after 3 months of dasatinib treatment (E). This dog remains alive 33 months after diagnosis.

treatment and survival data from four dogs given dasatinib as an adjuvant treatment for OS.

The study of metastatic behavior is complicated by the fact that some tumor cells may harbor one or more mutations that drive both metastasis and antiapoptotic or proliferative mechanisms. In this study, we used low-concentration TKI incubations ± HGF as a way to observe the HGF-specific behavior of cells in the presence of sublethal concentrations of TKI. Higher TKI concentrations may have had a greater effect, but it seemed implausible that dying cells would exhibit metastatic behavior. In this regard, HGF blocked the effects of dasatinib on viability at low drug levels, suggesting that the HGF pathway modulates both viability/proliferation and invasion in this model system. However, the absence of an increase in cell death or

apoptosis in response to 20 nM dasatinib (Figure 4) suggests that dasatinib is primarily antiproliferative at low drug levels. In the current study, we attempted to delineate between metastatic and proliferative behaviors *in vitro*; however, the fact that TKI incubation affects multiple physiologic pathways is important, and further studies that seek to elucidate these differences are warranted.

HGF increased the rate of migration and invasion in both cell lines tested. Similarly, both cell lines appeared to have constitutive activation of the MET RTK at tyrosines 1230, 1234, and 1235, which are in an activating kinase domain. Incubation with low-concentration crizotinib, which is reported to be a MET-specific TKI, or dasatinib did not significantly reduce the apparent phosphorylation of MET at these sites. Future studies might benefit

by determining the extent and cause of the autophosphorylation of MET in OS.

We were surprised that crizotinib but not dasatinib reduced the HGF-induced secretion of active MMP-9 in the COS cell line. Furthermore, there was no MMP-9 secretion detected from the Clone-4 cells; yet the cells were presumably able to degrade the invasion chamber substrate at the same rate as COS. We did not directly assess the mechanism of protease activity in the invasion model system but speculate that the Clone-4 cells depend on MMP-2 activity whereas the COS cells may achieve the same result using MMP-9. Regardless, the present data show for the first time that OS cells are able to secrete different forms of protease and these may function to degrade extracellular matrix and facilitate invasion.

Our inability to show a difference in MET phosphorylation upon activation with HGF suggests that HGF activated either a different RTK or a different epitope of MET. HGF exists as an alpha- and beta-chain heterodimer that can be cleaved into its component parts. Ohnishi et al. [19] recently identified a new receptor for the beta-chain of HGF (HGF-β), but this receptor was not investigated in the current study. Further study is warranted to advance our understanding of the mechanisms of HGF activation in OS.

The reported median survival time for dogs with appendicular OS treated with amputation and carboplatin is approximately 10 months [20,21]. Although the *in vivo* data presented here are anecdotal, we feel that they help to inform the transition from *in vitro* investigations of dasatinib in canine OS to the clinical setting. We previously reported that 0.75 mg/(kg day) of dasatinib was tolerable and achieved clinically relevant blood levels of the drug [16]. We have now extended this to include three additional dogs that appear to have improved survival. The one surviving dog reported here has lived more than 3.2 times longer than the reported median survival time. This dog has lived with waxing and waning pulmonary metastases for most of this time. Seemingly, dasatinib has played a role in this longevity. Although originally developed as a Src inhibitor, dasatinib is now known to affect multiple kinases, each with a broad range of functions. In this regard, dasatinib has been investigated for its capacity to reduce the permissive effects of T-regulatory immune cells in the tumor microenvironment [22–24]. We speculate that this could be important to canine OS and feel that the current observations, coupled with an acceptable dose and schedule for dasatinib administration, provide a basis for a clinical trial in dogs with OS.

Conflicting Interests

The authors declare no competing interests.

Acknowledgements

References

[1] Andermarcher E, Surani MA, and Gherardi E (1996). Co-expression of the HGF/SF and c-met genes during early mouse embryogenesis precedes reciprocal expression in adjacent tissues during organogenesis. *Dev Genet* **18**(3), 254–266.

[2] Schmidt L, Duh FM, Chen F, Kishida T, Glenn G, Choyke P, Scherer SW, Zhuang Z, Lubensky I, and Dean M, et al (1997). Germline and somatic mutations in the tyrosine kinase domain of the MET proto-oncogene in papillary renal carcinomas. *Nat Genet* **16**(1), 68–73.

[3] Rong S, Segal S, Anver M, Resau JH, and Vande Woude GF (1994). Invasiveness and metastasis of NIH 3T3 cells induced by Met-hepatocyte growth factor/scatter factor autocrine stimulation. *Proc Natl Acad Sci U S A* **91**(11), 4731–4735.

[4] Gherardi E, Birchmeier W, Birchmeier C, and Vande Woude G (2012). Targeting MET in cancer: rationale and progress. *Nat Rev Cancer* **12**(2), 89–103.

[5] Tseng JR, Kang KW, Dandekar M, Yaghoubi S, Lee JH, Christensen JG, Muir S, Vincent PW, Michaud NR, and Gambhir SS (2008). Preclinical efficacy of the c-Met inhibitor CE-355621 in a U87 MG mouse xenograft model evaluated by 18F-FDG small-animal PET. *J Nucl Med* **49**(1), 129–134.

[6] Michieli P, Mazzone M, Basilico C, Cavassa S, Sottile A, Naldini L, and Comoglio PM (2004). Targeting the tumor and its microenvironment by a dual-function decoy Met receptor. *Cancer Cell* **6**(1), 61–73.

[7] Logan TF (2013). Foretinib (XL880): c-MET inhibitor with activity in papillary renal cell cancer. *Curr Oncol Rep* **15**(2), 83–90.

[8] Grullich C (2014). Cabozantinib: a MET, RET, and VEGFR2 tyrosine kinase inhibitor. *Recent Results Cancer Res* **201**, 207–214.

[9] Stellrecht CM and Gandhi V (2009). MET receptor tyrosine kinase as a therapeutic anticancer target. *Cancer Lett* **280**(1), 1–14.

[10] Sampson ER, Martin BA, Morris AE, Xie C, Schwarz EM, O'Keefe RJ, and Rosier RN (2011). The orally bioavailable met inhibitor PF-2341066 inhibits osteosarcoma growth and osteolysis/matrix production in a xenograft model. *J Bone Miner Res* **26**(6), 1283–1294.

[11] McCleese JK, Bear MD, Kulp SK, Mazcko C, Khanna C, and London CA (2013). Met interacts with EGFR and Ron in canine osteosarcoma. *Vet Comp Oncol* **11**(2), 124–139.

[12] Fieten H, Spee B, Ijzer J, Kik MJ, Penning LC, and Kirpensteijn J (2009). Expression of hepatocyte growth factor and the proto-oncogenic receptor c-Met in canine osteosarcoma. *Vet Pathol* **46**(5), 869–877.

[13] De Maria R, Miretti S, Iussich S, Olivero M, Morello E, Bertotti A, Christensen JG, Biolatti B, Levine RA, and Buracco P, et al (2009). met oncogene activation qualifies spontaneous canine osteosarcoma as a suitable pre-clinical model of human osteosarcoma. *J Pathol* **218**(3), 399–408.

[14] McCawley LJ, O'Brien P, and Hudson LG (1998). Epidermal growth factor (EGF)– and scatter factor/hepatocyte growth factor (SF/HGF)–mediated keratinocyte migration is coincident with induction of matrix metalloproteinase (MMP)-9. *J Cell Physiol* **176**(2), 255–265.

[15] Wang H and Keiser JA (2000). Hepatocyte growth factor enhances MMP activity in human endothelial cells. *Biochem Biophys Res Commun* **272**(3), 900–905.

[16] Davis LE, Hofmann NE, Li G, Huang ET, Loriaux MM, Bracha S, Helfand SC, Mata JE, Marley K, and Mansoor A, et al (2013). A case study of personalized therapy for osteosarcoma. *Pediatr Blood Cancer* **60**(8), 1313–1319.

[17] Shor AC, Keschman EA, Lee FY, Muro-Cacho C, Letson GD, Trent JC, Pledger WJ, and Jove R (2007). Dasatinib inhibits migration and invasion in diverse human sarcoma cell lines and induces apoptosis in bone sarcoma cells dependent on SRC kinase for survival. *Cancer Res* **67**(6), 2800–2808.

[18] Marley K, Helfand SC, Edris WA, Mata JE, Gitelman AI, Medlock J, and Seguin B (2013). The effects of taurolidine alone and in combination with doxorubicin or carboplatin in canine osteosarcoma in vitro. *BMC Vet Res* **9**, 15.

[19] Ohnishi H, Oka K, Mizuno S, and Nakamura T (2012). Identification of mannose receptor as receptor for hepatocyte growth factor beta-chain: novel ligand-receptor pathway for enhancing macrophage phagocytosis. *J Biol Chem* **287**(16), 13371–13381.

[20] Phillips B, Powers BE, Dernell WS, Straw RC, Khanna C, Hogge GS, and Vail DM (2009). Use of single-agent carboplatin as adjuvant or neoadjuvant therapy in conjunction with amputation for appendicular osteosarcoma in dogs. *J Am Anim Hosp Assoc* **45**(1), 33–38.

[21] Bergman PJ, MacEwen EG, Kurzman ID, Henry CJ, Hammer AS, Knapp DW, Hale A, Kruth SA, Klein MK, and Klausner J, et al (1996). Amputation and carboplatin for treatment of dogs with osteosarcoma: 48 cases (1991 to 1993). *J Vet Intern Med* **10**(2), 76–81.

[22] Fei F, Yu Y, Schmitt A, Rojewski MT, Chen B, Gotz M, Dohner H, Bunjes D, and Schmitt M (2009). Dasatinib inhibits the proliferation and function of CD4+CD25+ regulatory T cells. *Br J Haematol* **144**(2), 195–205.

[23] Yang Y, Liu C, Peng W, Lizee G, Overwijk WW, Liu Y, Woodman SE, and Hwu P (2012). Antitumor T-cell responses contribute to the effects of dasatinib on c-KIT mutant murine mastocytoma and are potentiated by anti-OX40. *Blood* **120**(23), 4533–4543.

[24] Kreutzman A, Ilander M, Porkka K, Vakkila J, and Mustjoki S (2014). Dasatinib promotes Th1-type responses in granzyme B expressing T-cells. *Oncoimmunology* **3**, e28925.